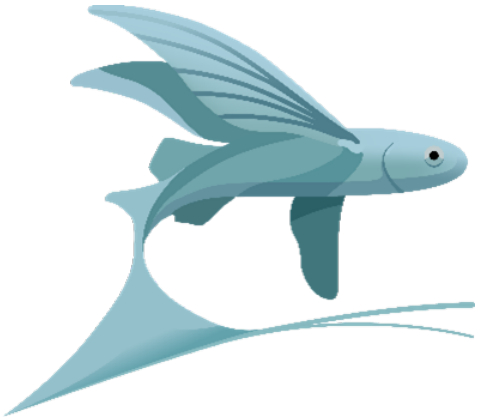


# ESTACA WAVE Team

Laval, France

**Sumoth Challenge 2024**

Stage S1 - Boat Design

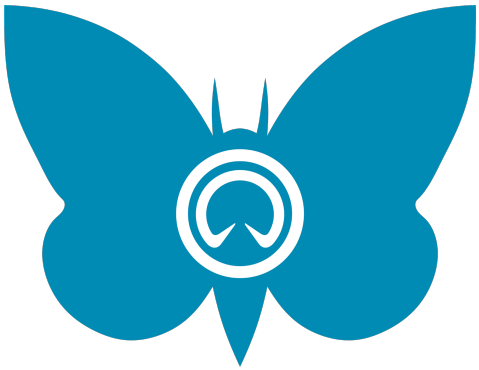

Monday 20th May, 2024

**Abstract**

This paper presents the progress and findings of a team of transport engineering students from ESTACA engaged in the innovative SUMoth (Sustainable Moth) challenge. Initiated in 2022, our team embarked on the ambitious journey to design and construct a sustainable foiling sailboat. The challenge, spanning multiple stages, demands ingenuity in engineering, sustainability, and performance optimization. As of the S1 stage, we have laid the foundation for our endeavor, with the boat's mold meticulously crafted and construction well underway. This report outlines the key methodologies employed, including materials selection, design considerations, and sustainability initiatives. Additionally, we discuss the challenges encountered and the strategies devised to address them. Looking ahead, our team is eager to continue the journey, with the aspiration of showcasing our fully realized, sustainable foiling sailboat in the upcoming competition. Through this project, we aim not only to learn in the challenge but also to contribute to the advancement of sustainable transportation solutions in the maritime domain.

# Contents

# List of Figures

# Chapter 1

# Engineering and design

## 1.1 Hull design principles

The design of the hull was one of the most challenging step in the first part of the project. Indeed, as it is the starting point for all further steps, first design iterations began at the very beginning. To start designing an object, one should first start thinking about the objectives and the way it will be used and built. The hull will have to be light and generate the lowest achievable drag during takeoff and flight. Moreover, its buoyancy should allow the boat to float in all situations. To finish, as our team has no experience in composite manufacturing, our hull has been designed in order to be manufactured as easy as possible.

| General design parameters | | |
|---|---|---|
| Optimized drag hull displacement | 70 | [L] |
| Static displacement | 110 | [L] |
| T | 15.24 | [cm] |
| Takeoff speed | 6 | [kt] |
| CP | 0.65 | [] |
| Takeoff Froude number | 0.7 | [] |

To begin, the team has studied various moth hulls to better understand the essential parameters for designing an efficient hull. Some modern designs are particularly noteworthy from an aerodynamic perspective, exhibiting reduced windage drag, which indicates signifi-

cant optimization efforts aimed at enhancing maximum speed. However, our team chose to draw inspiration from older moths, constructed with heavier structures due to the material limitations imposed by the challenge. For these reasons, we decided to retain the following initial parameters based on the paper "Full Scale Measurements on a Hydrofoil International Moth" published by Bill Beaver and John Zseleczky.

### 1.1.1 Hull shape

The first design constraint pertains to buoyancy: the boat must remain afloat under all conditions, requiring an estimation of its weight to determine the necessary displacement value. Consequently, the hull's minimum volume should be approximately 110 liters, accommodating a skipper weighing up to 85 kg. The second objective is to design a hull with minimized drag during the take-off phase, enabling the boat to fly even at low wind speeds. According to W. Henschke, hull drag can be reduced by varying the sectional area in a specific manner, depending on the Froude number, hull length, displacement, and prismatic coefficient.

$$Cp = \nabla/(A_x L)$$

The main objective of the hull shape is to reduce the drag during the take-off, when the foils already generate lift, and when the hull displacement is only about 70 liters. This displacement value has been set as an input in the maximum sectional area of the hull with Cp=0.65.

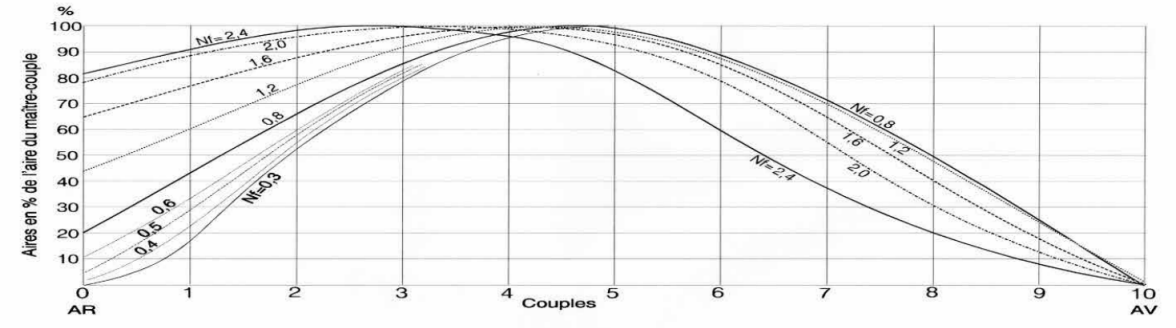


Figure 1.1: Sectionnal aera curves for different Froud numbers according to W. Henscke

With the general lines defined, the team created a fully parametric design using a CAD software, allowing numerous iterations and an easy integration with other boats components.

The sectionnal aera curve is fully respected and the hull satisfy all design requirements.

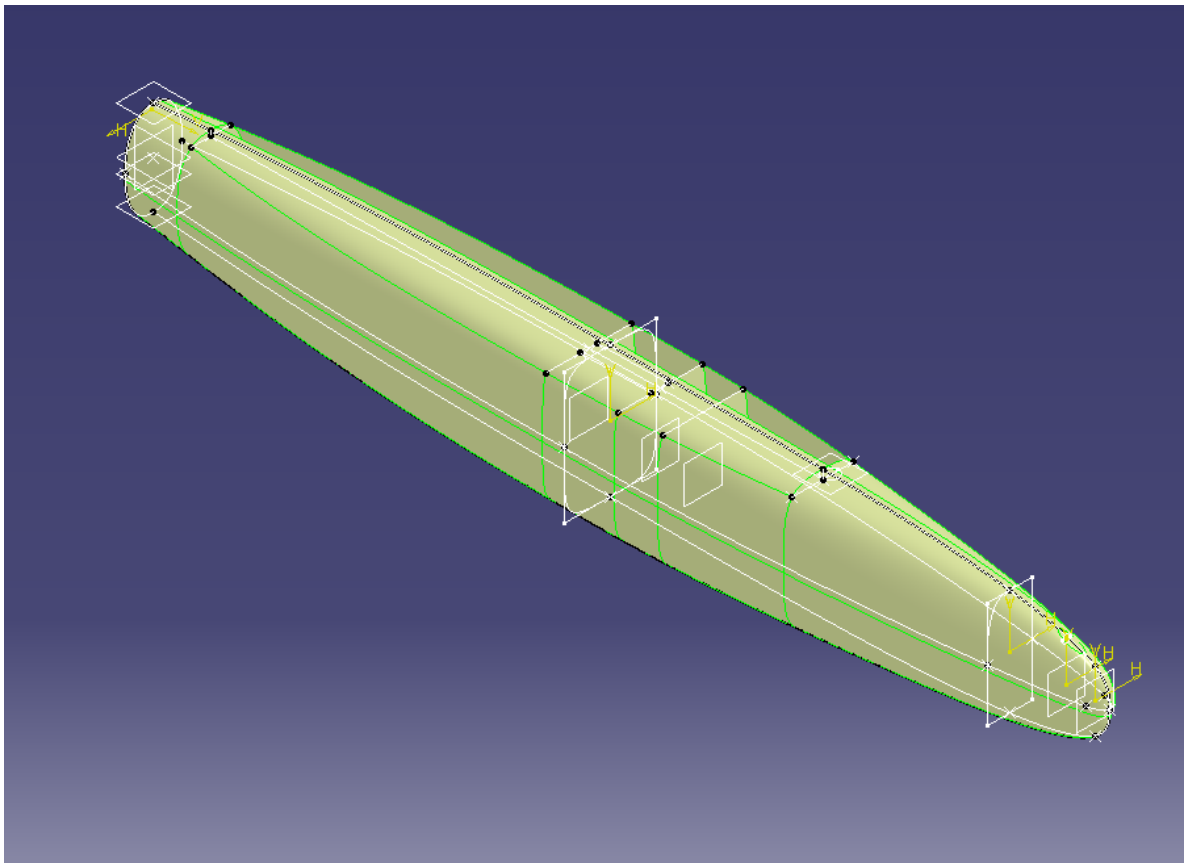

Figure 1.2: General overview of the hull shape

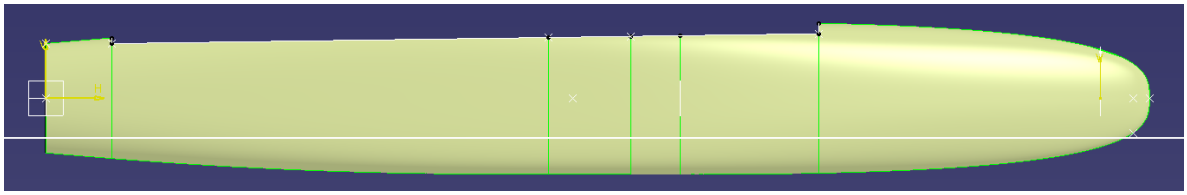

Figure 1.3: Side view of the hull with the takeoff floating line

To improve the carbon footprint and simplify the hull's manufacturing process, it is important to note that the hull exhibits complete symmetry along the horizontal plane. This symmetry allows the team to use a single mold for the entire hull, while maintaining a perfect sectional area curve.

### 1.1.2 Terraces

The focus now shifts to the design of the terraces, conceived as rigid wings. This innovative approach, being a first, presents challenges in terms of manufacturability, final weight, and integration onto the hull. The implementation of rigid wings required selecting a straightforward design, encompassing specific dimensions and angles. To achieve an optimal balance between ease of handling and competitiveness, input was obtained from an experienced skipper, whose insights informed the following design:

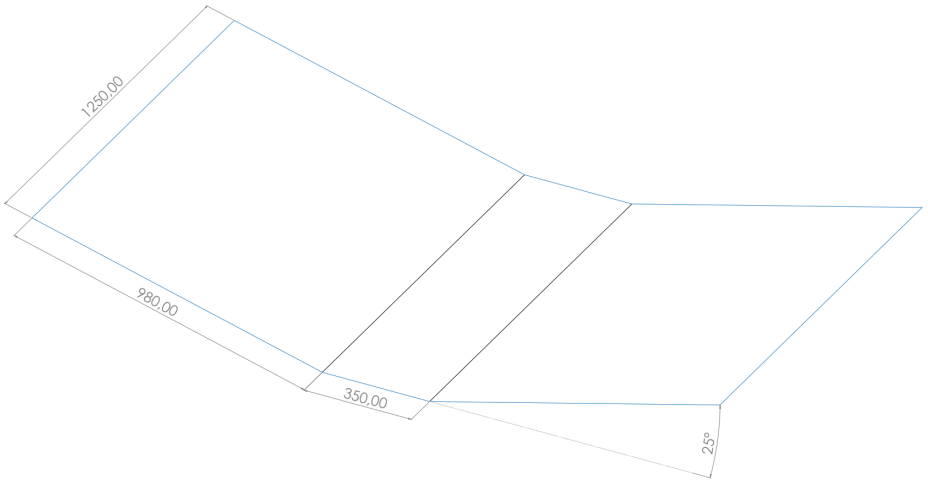


Figure 1.4: Terraces design

First of all, the wingbars will be straight as the trampoline will be a sandwich composite, which is easier to make with a flat mould. We chose to exploit the widest authorised wings width (2.25m) to benefit from the moment created from them. The deck is a bit wider than the hull and is 35cm wide, and the terraces lenght is 1.25m. The skipper told us that we could have reduced it to 1m, but it would have been harder to sail, so we decided to remain on our initial value. Finally, the wings angle is 25°, as it is on WASPZ boats. We primarily chose an angle of 15°, but once again, the result was that is wast enough steep, and that the manoeuvre angles wouldn't be big enough.

### 1.1.3 Gantry

Another structural element to be designed and manufactured is the foil frame, the structural component linking the hull to the rudderfoil. The design of the frame will be iterative until we come up with a design that suits us. In fact, we first thought of an asymmetrical design as described below, so as to have more fixing points and therefore more rigidity.

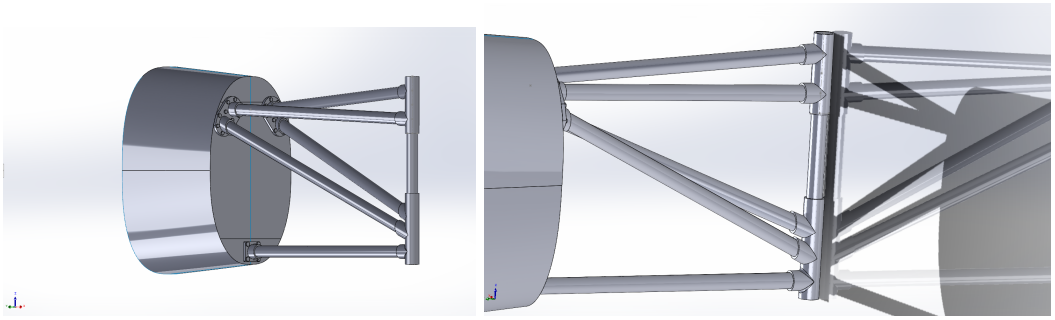

Figure 1.5: First version of the gantry

But fearing that using such a design would also generate asymmetrical efforts. After several iterations, we came up with the following design:

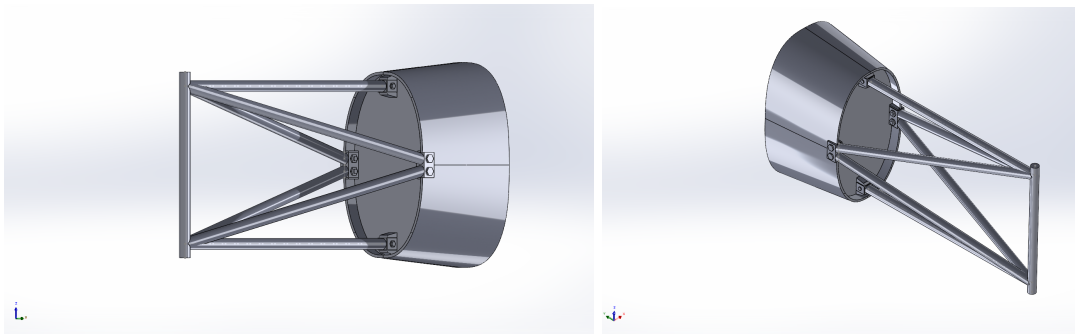

Figure 1.6: Final version of the gantry

This design finally consists in a symmetrical gantry, to be fitted around the perimeter of the rear panel. In fact, as we planned to move the panel inside of the hull (matching the required dimensions), we can expect the gantry to be fixed on the the outside part of the hull without degrading its mechanical strength.

## 1.2 Materials tests

During the preliminary design phase of the Moth, materials were selected to meet the primary objectives of the FSMC, prioritizing innovation, ecological impact, and competitiveness. The materials needed to have a low carbon footprint and strong mechanical properties. The initial stage involved researching potential materials, followed by structural testing to compare theoretical and experimental results to identify the best combinations.

The material selection process considered the fact that the team comprises students who share workshop space with other student associations, making safety a primary concern. Due to the known VOC emissions from composite materials, bio-based epoxy was used exclusively, as it is safer than acrylic resins, despite potentially being less sustainable. The guiding principle was that substances harmful to human health are also detrimental to the environment, a consideration maintained throughout the design phase.

The selection of materials was informed by the report from the 11th Hour Racing Team, with detailed references available in the bibliography. For reinforcements, basalt fiber and flax fiber were tested—basalt fiber for its innovative and durable properties, and flax fiber for being a bio-based material primarily produced in Western Europe. Regarding resins, Greenpoxy 56 and InfuGreen 810 were evaluated; however, one was unsuitable for vacuum infusion, and the other was too costly. Consequently, LB2 Infusion Bio Resin from Easycomposite was chosen for manufacturing. Additionally, two bio-based core materials were used: cork and balsa wood.

### 1.2.1 Tensile tests

To obtain the data required for modeling in software, such as Young's modulus or tensile stress, quasi-static tensile tests were conducted at a speed of 2mm/min on monolithic composite sheets consisting of six plies of woven fibers weighing 220g/m$^2$ for both flax and basalt. Each test series comprised five tests performed on specimens oriented at 0/90° and ±45°, with standardized dimensions (cf. Appendix 1). These specimens were cut directly from the composite sheet using a 2D machining tool.

During the tensile tests, three parameters were measured: the applied force, displacement,

and deformation. To calculate the applied stress, the force was divided by the average cross-sectional area of the specimen using the formula:  = F/S. To determine the Young's modulus of the material, the stress-strain curve ( = f()) was plotted. According to Hooke's Law,  = E * , allowing for the calculation of the Young's modulus (E) by considering the linear portion of the curve (up to approximately 0.2 percent strain).

A series of three sets of tests was carried out. The first set tested flax fiber combined with GreenPoxy 56, the second set tested flax fiber with InfuGreen 810, and the final set tested basalt fiber with InfuGreen 810.

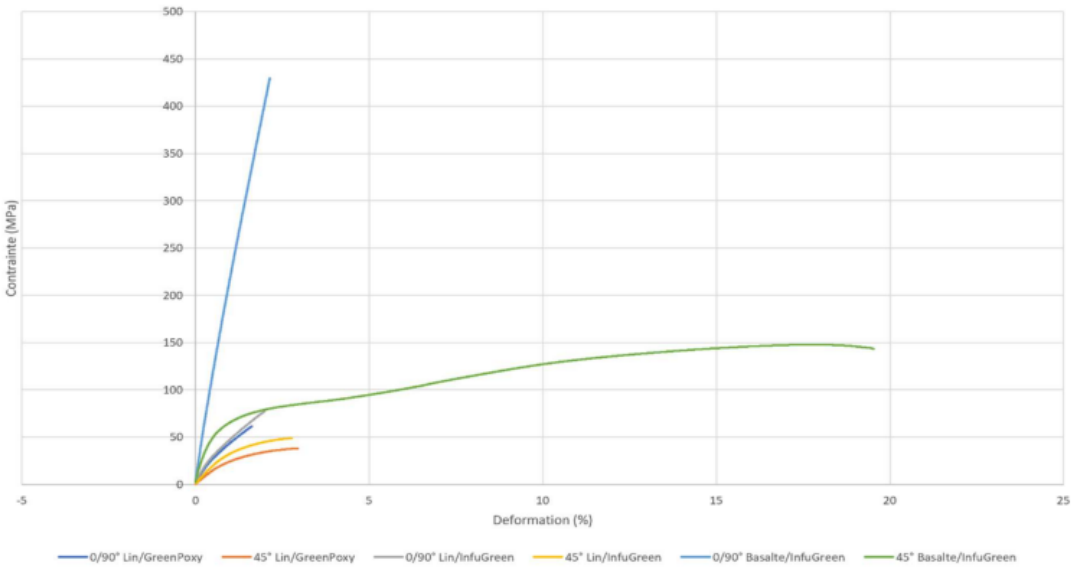


Figure 1.7: Tensile tests results

### 1.2.2 Bending tests

As the hull of a boat is primarily subjected to bending stresses, quasi-static bending tests were also conducted at a speed of 5mm/min. These tests were performed on sandwich composites similar to those used in previous years' SuMoth Challenge. The composite structure consisted of two plies (one oriented at 0/90° and one at ±45°) of the same monolithic weight on either side of a 5mm cork core. Unlike the tensile tests, only one series of five tests per composite plate was required for the bending tests. The dimensions of the specimens followed the ISO 14125 standard for 3-point bending (see Appendix 13).

During the bending tests, two parameters were measured: the applied force and the displacement, also known as deflection. The elongation was not measured. To calculate the

shear modulus, lateral displacement measurement would have been necessary. To obtain the bending stiffness of the material, the Force-Displacement curve (F = f(D)) was plotted, with stiffness given by K = F/D.

Two sets of tests were conducted. The first set tested flax fiber combined with Infu-Green 810 and a cork core. The second set tested basalt fiber with the same resin and core configuration, allowing for a comparative analysis.

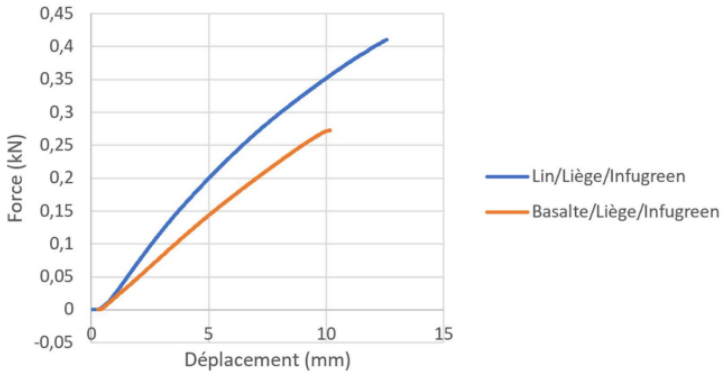


Figure 1.8: Bending tests results

### 1.2.3 Material choices

In terms of the mechanical tensile performance of fibres, basalt is much more attractive than flax, with a Young's modulus 4 times higher for half the weight. The lower performance in bending is not a problem, as the extreme lightness and low weight of a basalt fibre composite of a basalt fibre composite will allow us to add a few plies depending on the stresses that will be applied to the hull. Furthermore, the light weight of basalt due to its low resin absorption means that much less resin will be used, which is a real strength in terms of both competitiveness environmentally and financially. For example, we needed 700g of resin for a monolithic flax sheet, compared with monolithic sheet compared with 315g for a basalt sheet, which represents a weight saving of 55 percents for a composite sheet. not insignificant on the scale of a boat. Another problem with linen is that it is unsuitable for use in aquatic environments, as it is very sensitive to humidity, which has a major impact on its lifespan. This is not the case with mineral fibres such as basalt. Note that our results are very similar to those found by Ghent University for the same tests (see Ghent report). Given the time available, our choice of materials can be summarised as follows: The shell (excluding partitions) will be

defined by a stack of 0/90 and +/-45 plies of BAS 220 Twill on a 5 mm thick cork core. UD strips will reinforce certain areas subject to high tensile stress. The same reinforcement will be used for bulkheads and flat areas, but the core will be made of 6.5 mm balsa wood. The center of terraces is made from recycled PET foam.

## 1.3 Structural study

### 1.3.1 Static analysis

Before carrying out any structural study on the various elements of the boat, it is necessary to determine the forces which apply to them, as well as the dimensioning load case which will ensure that all the other load cases hold. An initial study was carried out last year to determine the maximum buoyancy provided by the wind when sailing close-hauled, i.e. at 20° to the wind. However, we didn't take the time at the start of the year to isolate the hull and decks to carry out the Fundamental Principle of Statics (FPS), which didn't give satisfactory results. Calculating the forces and moments on the insulated parts should therefore have been our priority at the start of the project.

#### 1.3.1.1 Dimensioning load case

Among the various possible loading cases, we have summarised 4: with a skipper and wind, with a skipper with no wind, without a skipper with wind in the case where the skipper is in the water and finally, with no wind and no skipper. It turns out that the dimensioning case is the case where the skipper is on the moth in the presence of wind. For all subsequent studies, a safety factor of 4 will be used to consider the case of a crash, for example, where the boat is subjected to a severe test. The forces acting on the boat system are summarised below:


Figure 1.9: Forces applying of the moth hull

For the system to be static, the forces must compensate each other. There are 3 types of force acting on a moth: aerodynamic and hydrodynamic forces, rigging tension and the weight of the boat and skipper. The lift of the foils (whose distribution is not yet known) is equal to the weight of the boat and skipper, i.e. around 1200N. The drag of the foils is equal to the 2800N of buoyancy. Finally, the compression force on the mast results from the pre-tension of the forestay and the two shrouds, of 2000N and 2x 1800N respectively.

The definition of these forces allows us to deduce the value of the unknown forces involved in the boat system. However, to study the staticity of the hull, we need to study it in isolation, without considering any external forces. To achieve this in a simple way, we carried out 3 studies involving the 3 types of forces mentioned above. The unknown forces to be found are the distribution of the lift, drag and anti-drift forces of the foils, the stresses applied to the hull by the decks and, finally, the resultant at the foot of the mast of the rig tension.

#### 1.3.1.2 Aero and hydro forces

To determine the distribution of foil forces, we focused our study on the aero and hydro forces acting on the moth.We therefore produced a Matlab code (see appendices) to determine their lift, drag and anti-drift force, the unknowns in the 6 equations given by the FPS ($\Sigma F = 0$ and $\Sigma M = 0$).To determine the force $L_{sail_y}$ exerted along y by the sail, a simple equilibrium with the skipper is sufficient such that the moment created between this force and the point of application-sail distance is equal to the moment created between the skipper's weight $W_{crew}$ and the skipper-hull distance.

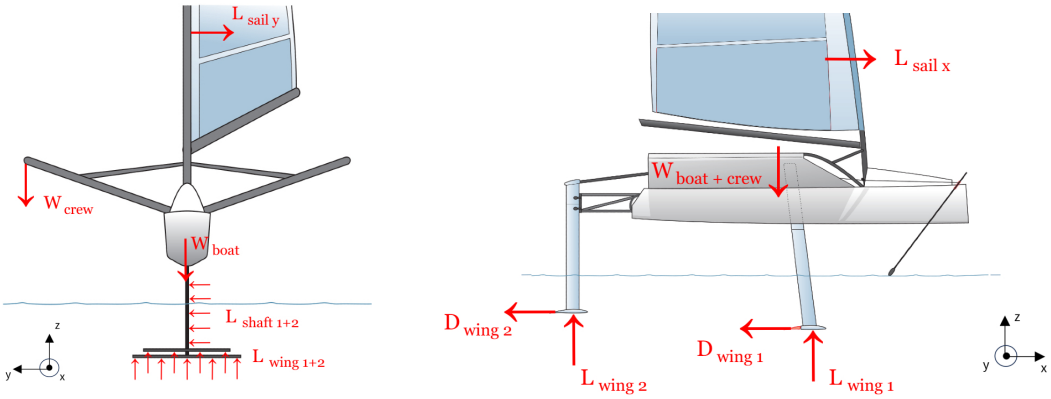


Figure 1.10: Aero and hydro forces applying on a moth

However, it turned out that the system was coupled, and that one of the equations was a linear combination of another. To reduce the number of unknowns to 5, we assumed that the drag of the rudder foil was half that of the main foil.This is because drag is defined by : $D = \frac{1}{2}\rho V^2 S C_x$ and in our case, only the surface area of the foils changed with $S_{foil} = 0.067m^2$ and $S_{rudder} = 0.034m^2 \cong \frac{1}{2}S_{foil}$. We then obtain the following rounded forces, coefficient 4 :

- Main foil drag $D_{wing_1} = 200N$ and therefore rudder foil drag $D_{wing_2} = 100N$,
- Main foil lift $L_{wing_1} = 3650N$ and rudder blade lift $L_{wing_2} = 1150N$,
- Anti-drift forces of main foil $L_{shaft_1} = 600N$ and rudder foil $L_{shaft_2} = 200N$.

Except for the drag, we can therefore see a $\frac{3}{4}$ / $\frac{1}{4}$ distribution of lift and anti-drift forces between the main foil and the rudder.

#### 1.3.1.3 Rig forces

Next, we want to determine the forces and moments that apply at the mast step, which we model by means of an embedment. These compressive forces result from the pre-tensioning of the rigging, i.e. the tension of the shrouds $T_{shrouds}$ and the forestay $T_{forestay}$. As these cables are also considered to be embedded in the decks, it is assumed that all the tension is applied to the mast.

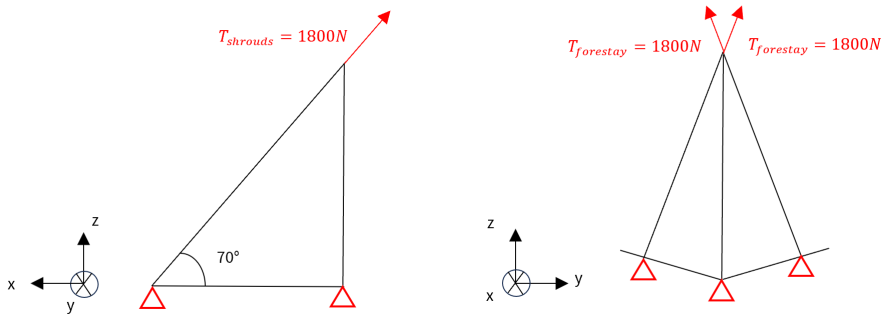


Figure 1.11: Forces applying of the mast

Once again, we performed a FPS using Matlab for this model, and the result is :

```
RX: -808.0
RY: 3030.161146640777587890625
RZ: -9469.540966033935546875
MX: 3084.381213665008544921875
MY: 2932.321199893951416015625
MZ: -978.391919970512390136718 75
```

#### 1.3.1.4 Terraces stresses

Finally, we want to determine the forces that apply to the hull at the deck attachment point. We proceed in the same way, isolating the deck system subject to the tension of the shrouds $T_{forestay}$ and the weight of the skipper $W_{crew}$. The system can then be modelled by a beam of width L embedded at its two ends :

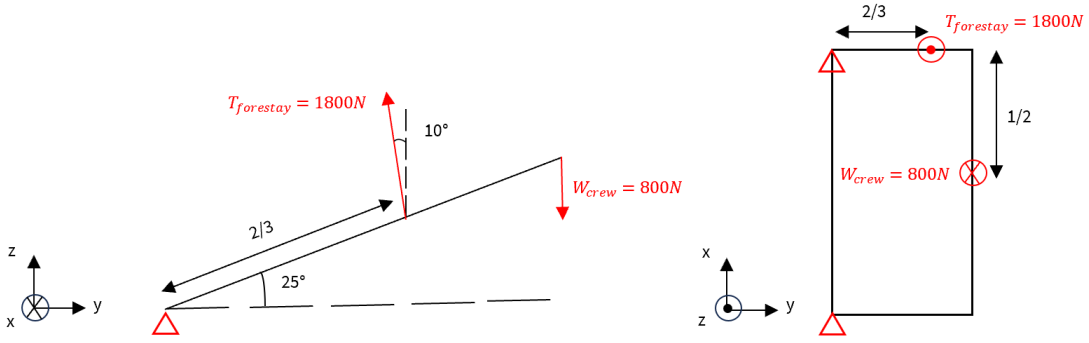


Figure 1.12: Forces applying of the terraces

In this case, but also in the finite element analysis of the hull, we will study the forces on one side of the decks and then symmetrise the results to simulate the case where the skipper is on the left side of the boat. By carrying out the FPS at embedding in the YZ plane, we obtain the following reactions:

```
RYO1: -2064.87517070770263671875
RZO1: -1379.347359454631805419921875
MXO1: -466.184840142726898193359375
RYO2: 0
RZO2: 1569.6
MXO2: 0
```

#### 1.3.1.5 Forces summary

Now that the preliminary FPS calculations have been carried out, let's summarise the forces and moments applied with the safety coefficient to our hull within the framework of the following FEM study. In order to obtain a symmetrical result for the two loadsteps by linear interpolation of the contours, the load case associated with a skipper on the left will be the same but symmetrised with the ZY plane.

| Norme | MAT | TERRASSES_AVANT_DROITE | TERRASSES_AVANT_GAUCHE | TERRASSES_ARRIERE_GAUCHE | TERRASSES_ARRIERE_DROITE | ETAI | RUDDER |
|---|---|---|---|---|---|---|---|
| RX | -808 | 2064 | -2064 | X | X | X | 192 |
| RY | 3030 | X | X | X | X | -2736 | -98 |
| RZ | -9475 | -1380 | -2948 | X | 1568 | 7517 | 1094.5 |
| MX | 3086 | X | X | X | X | X | X |
| MY | -1914 | 466 | 2322 | X | X | X | X |
| MZ | -978 | X | X | X | X | X | X |

Figure 1.13: Forces applying of the moth hull

### 1.3.2 Hull

#### 1.3.2.1 Challenges and objectives

The study of the hull using the "finite element method" forms the core of the engineering section. Before going into detail about the work undertaken, it is important to clearly and concisely describe the objectives and goals to be achieved. Ultimately, what we want to get out of the FEM analysis of the hull are: stress paths and various laminates likely to meet our mechanical and mass constraints.

The stress paths enable us to identify the areas where stress concentrations are highest, so that we can add more plies in these areas. The two laminates discussed below consist of an "infinite" laminate and a "Base&Rosace" laminate.

The first is characterized by particularly high ply thicknesses, the aim being to see what the software can offer by progressively reducing ply thicknesses at each iteration until displacement is minimized for a given maximum mass of 25kg. As for the second, it features a laminate made up of both the base laminate and a rosette oriented in all directions.

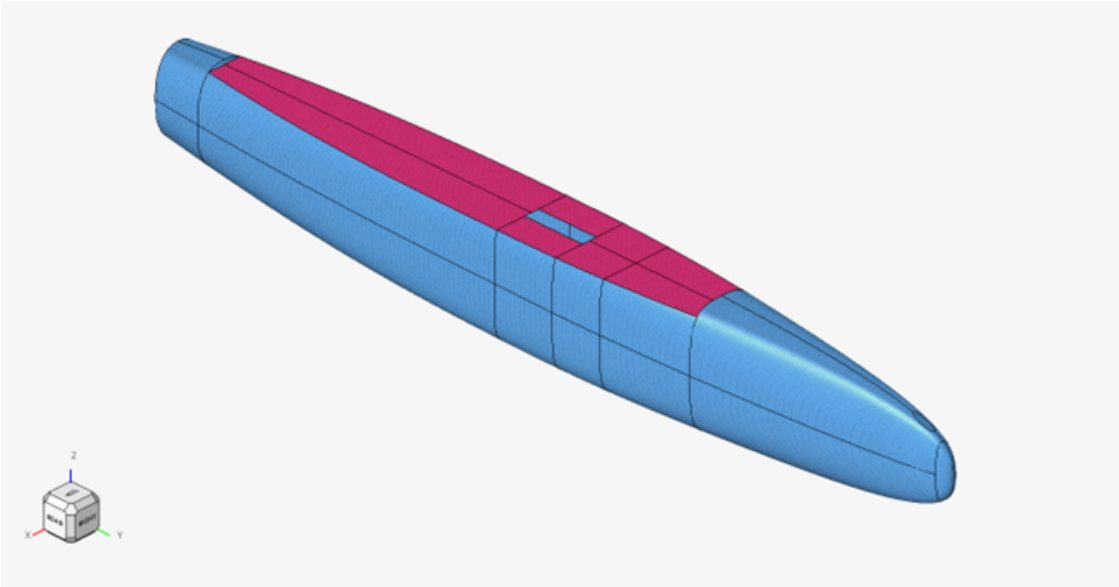

Figure 1.14: CAD model of the hull

#### 1.3.2.2 Summary of the steps involved in freesizing

In this section, we will discuss the various steps involved in any FEM problem, in order to arrive at a first set of results. Indeed, in the interests of brevity, we won't go into detail on all the steps that led us to the first exploitable results. In any FEM problem, we find the following steps:

- CAD model of the object of study,
- Definition and separation into elementary components of our model,
- Meshing the model,
- Definition of component properties,
- Definition of material properties,
- Definition of load cases,
- Definition of boundary conditions.

Below are a few images illustrating these sections.

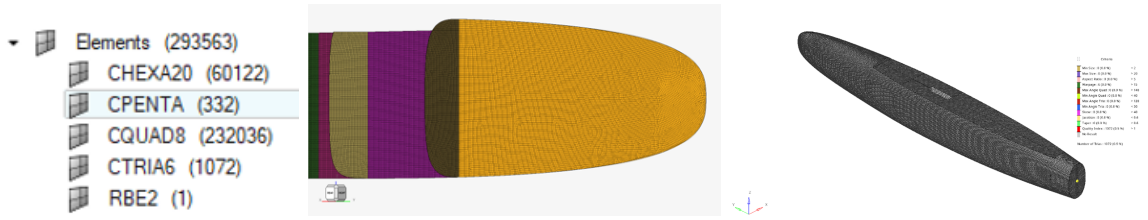


Figure 1.15: Meshing

| Name | ID | Include | Defined | Type | Card Image |
|---|---|---|---|---|---|
| STRATIFIÉ_VERRE | 1 | 0 | ☑ | ORTHOTROPIC | MAT8 |
| LIEGE_INFU | 2 | 0 | ☑ | ISOTROPIC | MAT1 |
| MAT_FOIL | 3 | 0 | ☑ | ISOTROPIC | MAT1 |
| BALSA_INFU | 4 | 0 | ☑ | ISOTROPIC | MAT1 |

| Materials | STRATIFIE_VERRE | LIEGE_INFUSE | MAT_FOIL | BALSA_INFUSE |
|---|---|---|---|---|
| E1 | 28730 | 3500 | 35000 | 21341 |
| E2 | 28730 | NA | NA | NA |
| NU12 | 0,13 | 0,21 | 0,13 | 0,3 |
| G12 | 4500 | 4,00E+01 | 10000 | 1000 |
| RHO | 1,84E-09 | 2,89E-10 | 0 | 2,77E-10 |
| XT | 85 | NA | 85 | NA |
| XC | 290 | NA | 290 | NA |
| YT | 85 | NA | NA | NA |
| YC | 290 | NA | NA | NA |
| S | 63 | NA | 63 | NA |
| CARTE_Matériau | MAT8 | MAT1 | MAT1 | MAT1 |

Figure 1.16: Materials and properties

#### 1.3.2.3 Analysis

Now it's time to run the analysis, using the -nt 8 and -core in commands to allocate the maximum ram to optistruct and give it access to 8 threads for calculation. We obtain the following results:

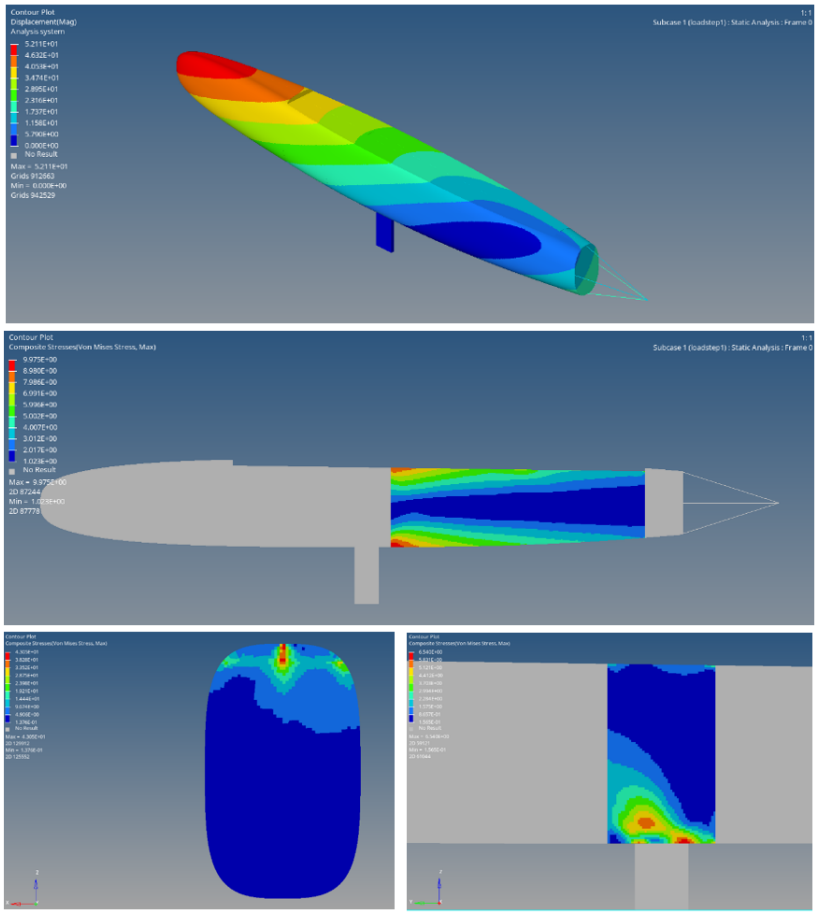

Figure 1.17: Analysis results

Maximum displacement is of the order of 5cm, which seems quite reasonable over several meters. What's more, the maximum stresses remain below the elastic stress of our composite. With these elements now known, we can now tackle the freesizing part of our study to find the stress paths and obtain the other two laminates discussed earlier.

#### 1.3.2.4 Determining force paths

Freesizing in MEF is a composite optimization operation which aims to iterate on the laminate until the design constraints are met. In this case, as in the next two, the optimization problem

will be parameterized in the same way: the aim is to minimize the displacement (from a node to the bow of the hull) while remaining below the 25kg threshold (hull + bulkheads).

In addition, we'll take care to parameterize our "variable design" as follows, in order to integrate manufacturability constraints such as minimum ply thickness or outward ply orientation:

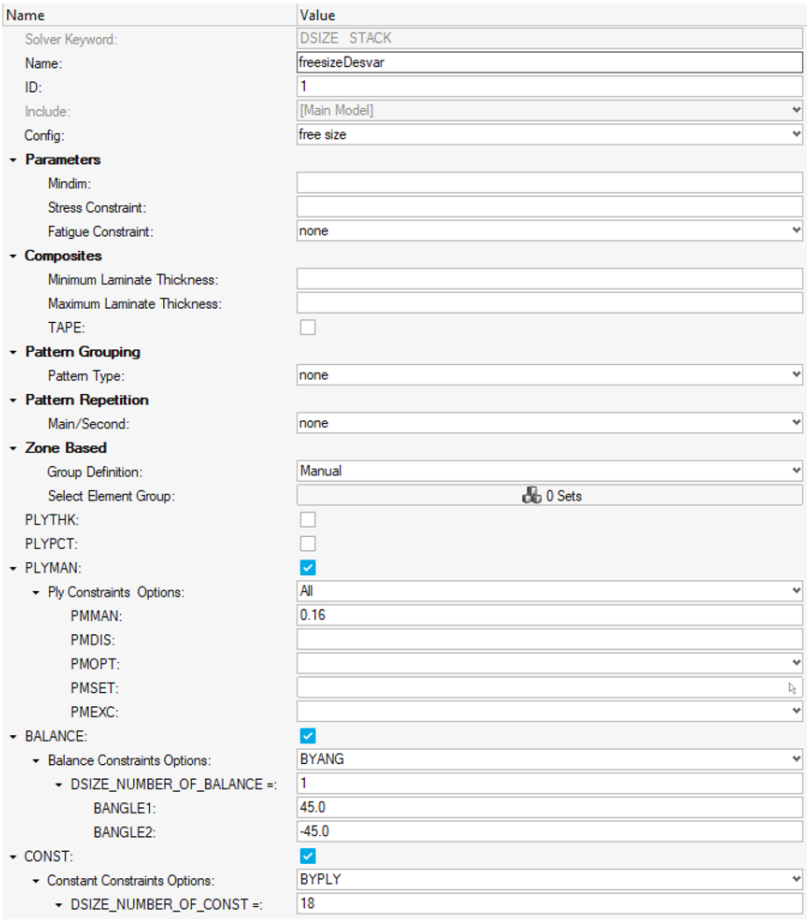


Figure 1.18: Freesizing parameters 2

To obtain the force paths, the method involves creating a laminate made up of plies ranging from 0 to 180 degrees, so as to create a "rosette". This laminate allows the stresses to pass through in any orientation, so that the result can be visualized as to where and in which directions the stresses are passing. Therefore, the following laminate will be used to create the rosette:

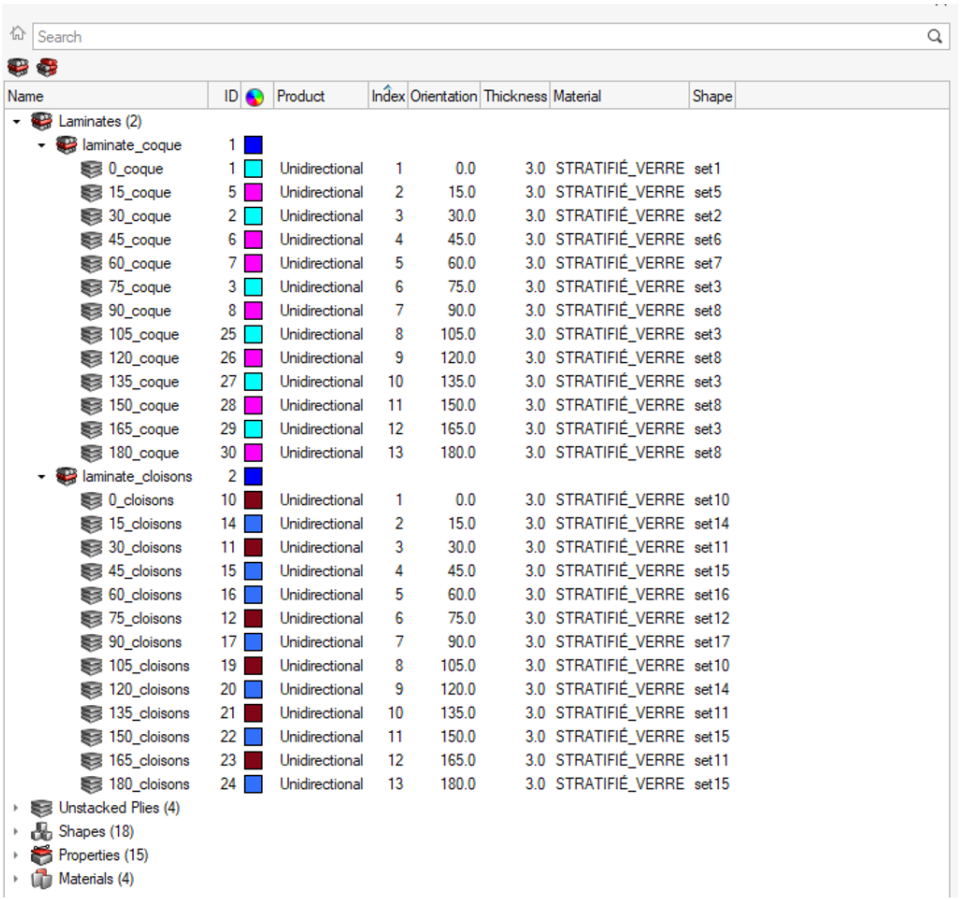


Figure 1.19: Rosette laminate for stress paths

To obtain a symmetrical result, we performed a linear superposition to obtain the envelope of forces on both loadcases (skipper on right and left). Once the freesizing optimization has been launched, we obtain the results below. We can see where stress concentrations are highest, corresponding to the areas where the freesizing optimization has decided to put the maximum amount of material.

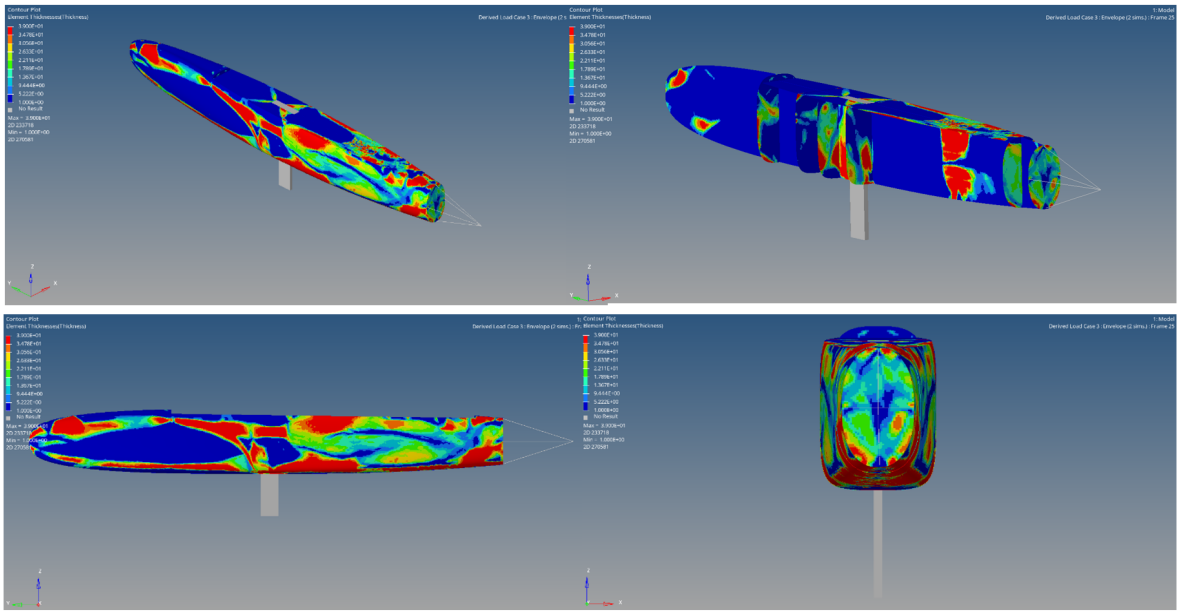

Figure 1.20: Freesizing rosace results

#### 1.3.2.5 Infinite laminate

In this second approach, the aim is to supply optistruct with our basic laminate, but with greater ply thicknesses. The software will then be able to provide us with a laminate proposal in line with the constraints described above. As detailed below, our "basic" laminate consists of 4 plies alternating between a 0/90,+/-45 orientation on each side of a 5mm and 6.4mm core for cork and infused balsa respectively.

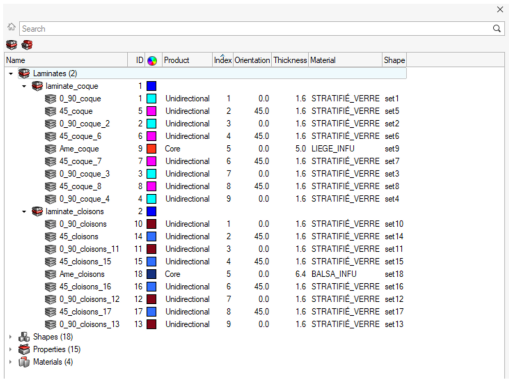


Figure 1.21: Infinite laminate

As previously mentioned, the folds are much thicker than usual. In fact, as indicated in the parameters of our "variable design", the TMANUF (minimum manufacturable thickness) is 0.16mm, i.e. 10x less than the ply thickness indicated in this case. It's important to note that in this case, the ply associated with the core has been completely blocked so that its thickness is not reduced during freesizing, and only the plies are optimized. With the above parameters and the laminate described above, we obtain the following results:

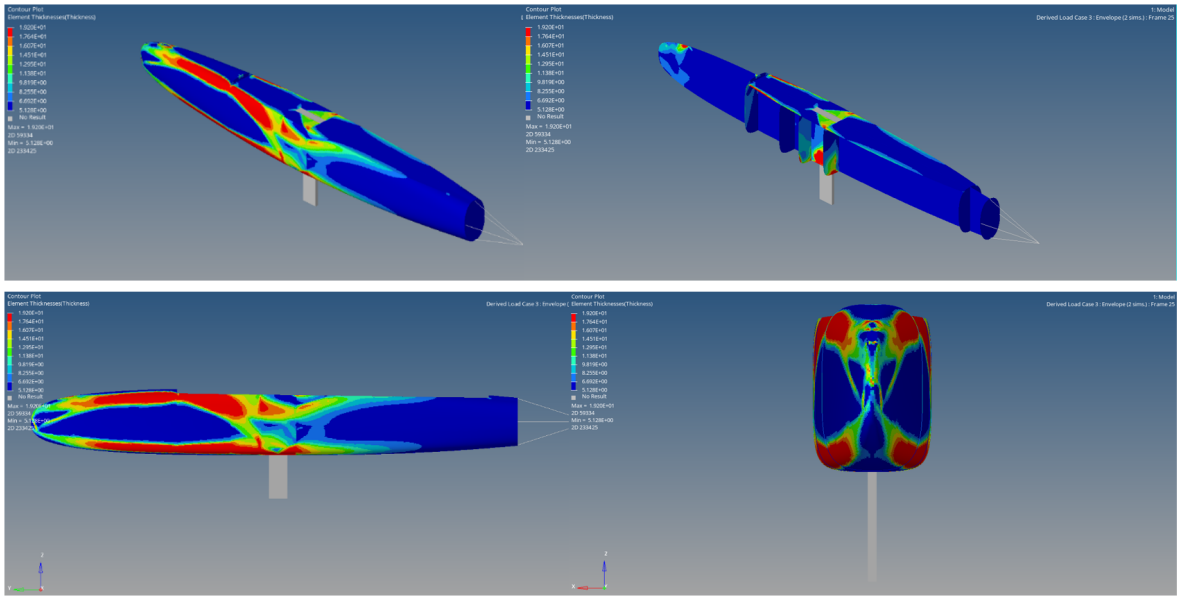

Figure 1.22: Infinite freesizing results

Similar to the previous rosette, but less precise in certain areas. In fact, optistruct once again tends to add material to the front of the hull on the upper and lower parts.

We can see that the use of folds ranging from 0 to 180 degrees gives greater precision in locating stresses, but it seems that the basic laminate is sufficient to take up these stresses, given that optistruct has decided not to reinforce the rear of the hull in particular.

#### 1.3.2.6 Base laminate and reinforcements

Finally, the aim of the 3rd laminate is to see what the software is capable of proposing if we wish to take the basic laminate and add a rosette of folds ranging from 0 to 180°, in order to identify the areas requiring additional folds, the thickness of these folds and their orientation. In the same way as we blocked the webs in the previous case, we will here block the entire base laminate so that optistruct, within the design constraints imposed on it, can find the optimum configuration for the reinforcement folds coming from the rosette. The laminate used for this study is summarized below:

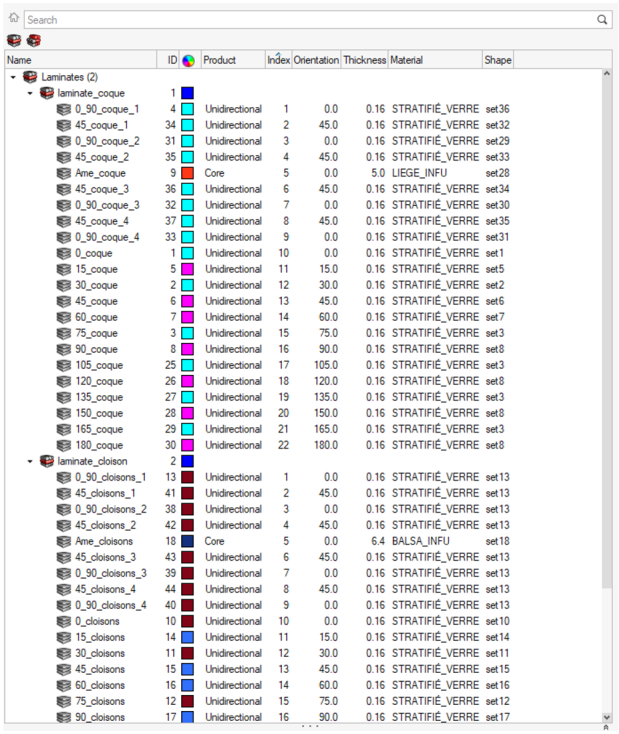


Figure 1.23: Basic laminate + reinforcements

This optimization gives us the following results:

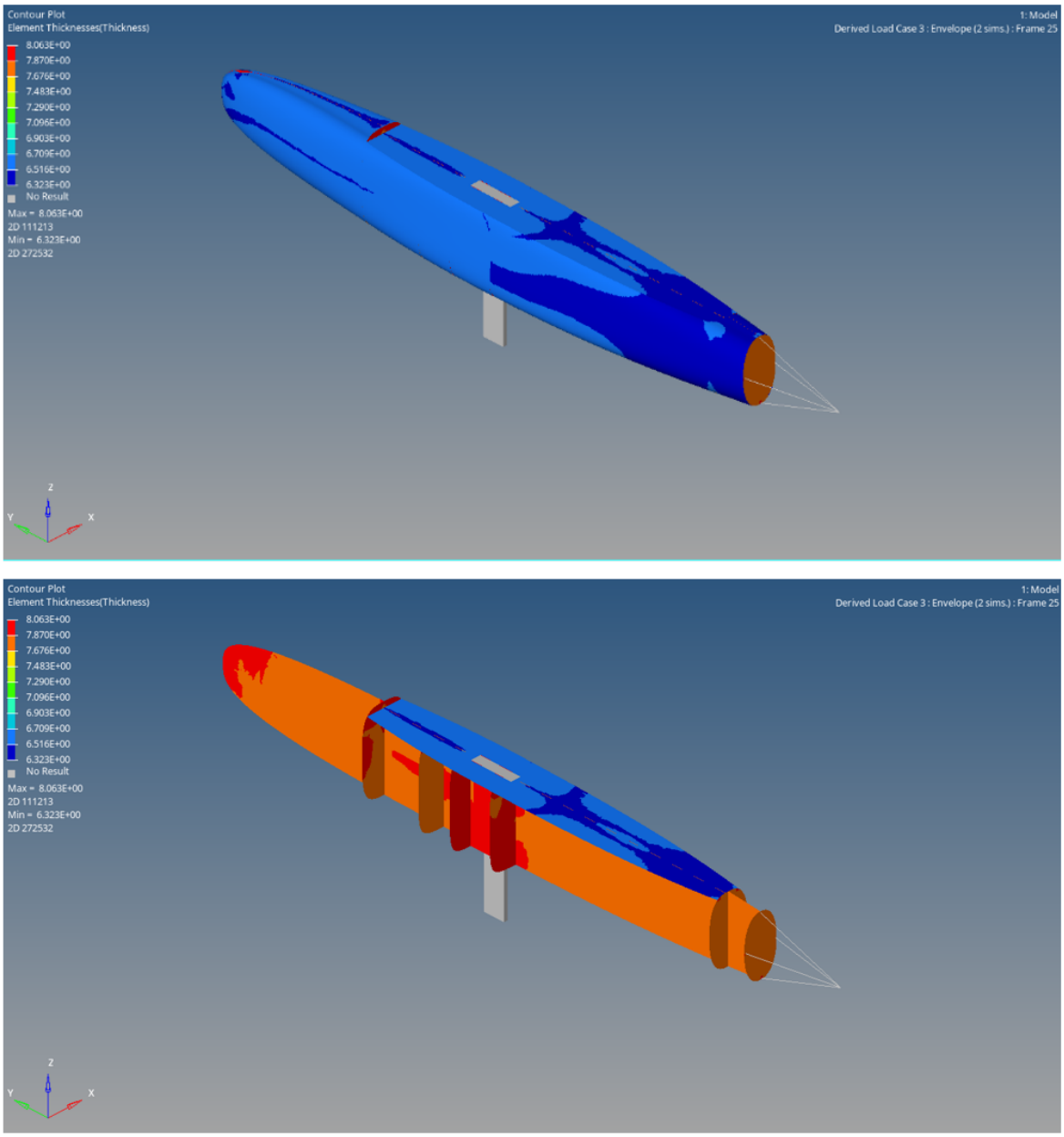


Figure 1.24: Results base + reinforcements

#### 1.3.2.7 Conclusion of MEF hull analysis

To conclude, let's summarize the various stages of thought that went into the MEF study of the hull.

As with any FEM project, it all began with the production of qualitative CAD models. These were then meshed into 2D & 3D quadratic elements, oriented and normalized. Once the meshing was complete, we set about defining our materials, properties, loadcases, subcases and, most importantly, our base laminate in 0/90,+/-45 .

All this led us to an initial analysis to judge the consistency of our results and the reaction of the hull (and therefore of our laminate) to the loadcase. Once we were satisfied, we decided to continue with the freesizing optimization, which enabled us to determine the precise stress paths, corresponding to where to place the UD fabrics, as well as two laminates that would help us to judiciously place the reinforcement plies during the construction phase.

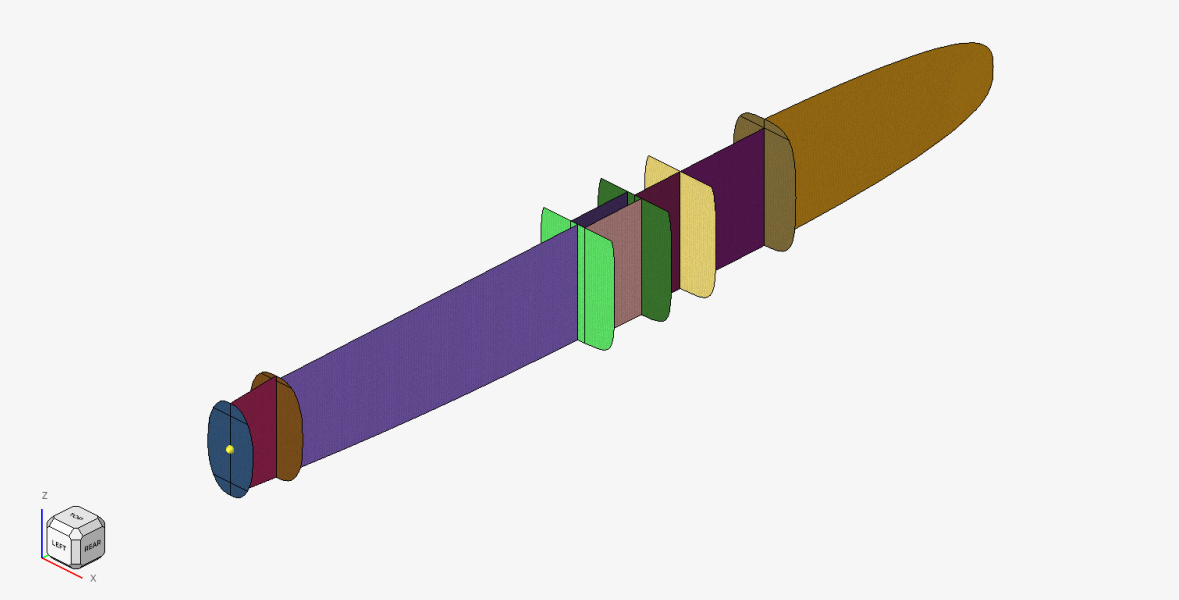

Figure 1.25: Hull model

### 1.3.3 Terraces

#### 1.3.3.1 Specifications

For the study of the wings, that we wanted being made of PET foam or balsa, we chose to study as previously stated the case where the skipper is located in the middle on the edge of one of the wings, creating an imbalance between the left side stretched upwards by the shroud and the right side counterbalanced by the skipper's weight. On top of that, we consider fixings at the 4 corners of the central deck, modelling its attachment to the hull. The study will be carried out with a safety coefficient of 4.

Before conceiving any model, we need to have an idea of the maximum weight we wanted to achieve. The advantage of solid wings is that they integrate the deck, usually around 1kg, the trampolines, around 2kg, and the wingbars into a single piece. In comparison with other teams, a competitive weight for wingbars would be around 10kg, which gives us a weight target of 13kg +/-10%, or just under 15kg at the upper limit.

#### 1.3.3.2 FEM analysis

As a first step, we tested wings made of sandwich composite over their entire surface area. Although their weight is not at all viable, this will enable us to understand the stress path in the full wing so that we can then optimise it manually.The result is the following thicknesses for the terraces seen from above, minimising displacement:

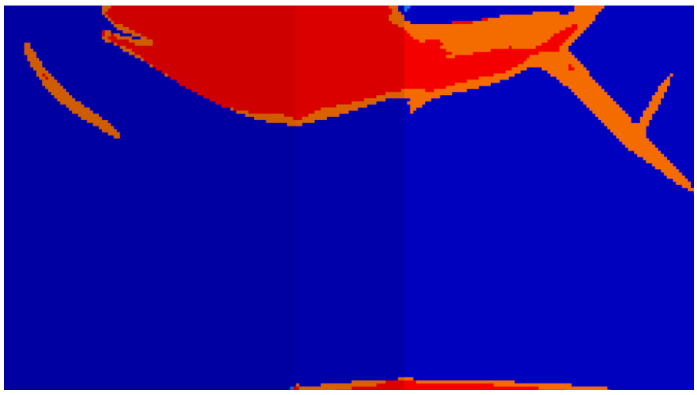

Figure 1.26: Wings free-sizing result

We can see that the software adds thickness in areas of high stress, i.e. at the points where the forces are applied (skipper's weight and shrouds), as well as at the bindings. In addition, we can see that these reinforcements connect these points of application to the bindings in the shortest possible way. Finally, it can be seen that the low-stress zones don't need any thickness compared with the high-stress zones. To satisfy our weight criteria and the conclusions drawn from the above analysis, we then designed our terraces with wingbars so that the core no longer covers the entire surface of the wing but only the contour of it.

In order to confirm these wings efficiency, we are going to compare them with the all-core wing model, both in terms of mass and displacement. We firstly studied different weights of the two models matching the sandwich composite criteria saying that the ratio core/skin must be between 10 and 100. It resulted in a mass divided by 2 or even by 3 for the thickest thicknesses, whatever the core material is, as balsa and foam have similar densities once infused (277kg/m3 and 212kg/m3). The most interesting core thicknesses for minimising weight seems therefore to be 40mm.

First of all, we observed that the moving zones are identical with or without wingbars. There is, however, a change of the displacement. With an all-balsa wing, which we can imagine is very stiff, the wing moves a maximum of about 2cm. For the model with balsa wingbars, the maximum point of movement is 5cm. On the other hand, the weight is also twice as light, dropping from 35 to 15kg. By way of comparison, for a all-foam wing of the same thickness, the displacement of the 2 models becomes 5cm and 13cm respectively. A foam wing, although a little lighter, therefore seems less stiff.

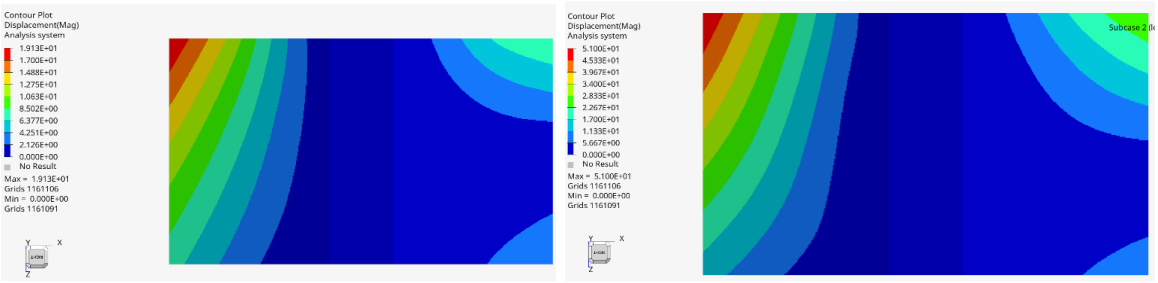


Figure 1.27: Wings made of balsa and PET foam wingbars displacement comparison

#### 1.3.3.3 Reduced scale tests

The only way to know whether a 5cm displacement is acceptable is to test the model, which we're going to do on a reduced 1:4 scale for ease of construction and cost.

##### 1.3.3.3.1 PET foam wings

Before talking about any bending tests, we first have to manufacture the composite part. Thanks to the previous material tests we did, we were able to pass on our skills in the infusion process to the rest of the team, while working independently in the lab. The first wing we made was composed of 10mm recycled PET foam wingbars and deck, all covered with 2 layers of 0/90 and +/-45 basalt on each side. For the bending test, we wanted to simulate shroud tension (in the opposite direction) by applying a force to one side of the deck and holding the deck as a fixture to the hull. Unfortunately, the test was disappointing and did not validate the displacement predicted for the force applied, i.e. 13cm for 1800N. Our impression of a general lack of stiffness in the part was therefore well-founded, and the test concluded with a failure at 3.5cm for 140N.

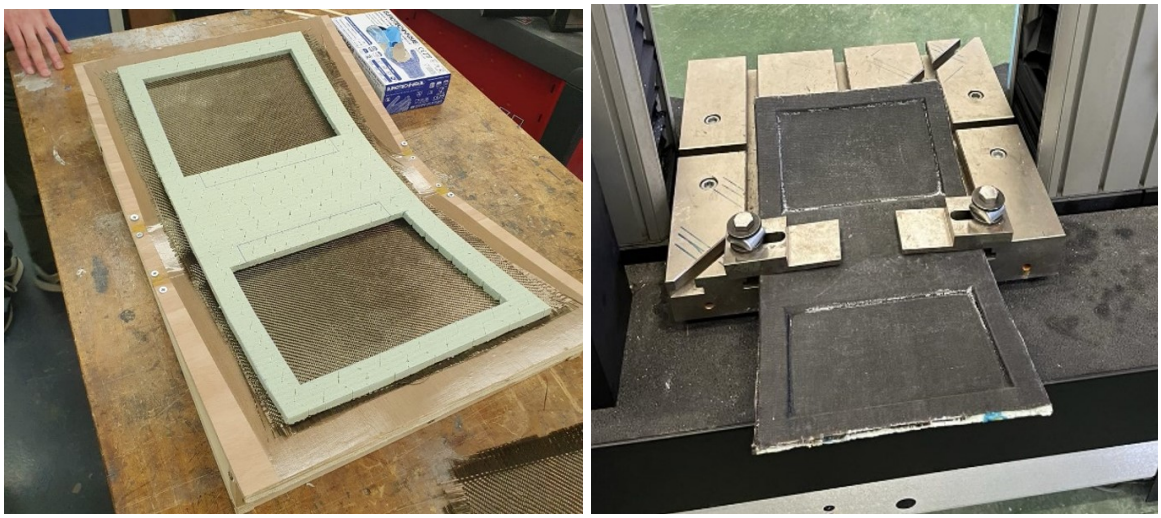

Figure 1.28: Construction and test of PET wings at 1:4 scale

In this configuration, the 1:4 scale wing weighs 406g, which seemed extremely light at first glance. However, as everything was designed to be 4 times larger in real life, the weight of the 1:1 scale is 0.406x64=26kg.

This weight doesn't meet our 15kg specification, which is why we decided to remove the core from the deck for the next test, as it doesn't absorb any stress. We as well concluded that the foam wasn't stiff enough for our purposes, unless we used a thicker layer, which would have been too heavy. Finally, We noticed that the failure occurred in the compression core at the junction between the wing and the deck. To try and increase stiffness, in other words compressive strength, we then tried balsa as the core material, one of the best bio-sourced materials for this type of stress.

#### 1.3.3.3.2 Balsa wings

In order to be able to compare the 2 tests, we only wanted to change one parameter, replacing the insufficiently stiff foam with balsa. However, many other parameters also had to be changed, which will prevent us from quantifying the immediate impact of this change of material. Among these changes, we noted that :

- the balsa was 6.4mm thick compared with 10mm for the foam,
- the balsa was pre-cut so the dimensions are not exactly the same,
- we removed a large part of the core on the deck.

In addition, after discussions with the team and moth specialists, we have modified the composite that acts as the deck and trampolines. In fact, we added a thin layer of 3mm foam to the monolithic composite to make it more resistant to compression and impact:

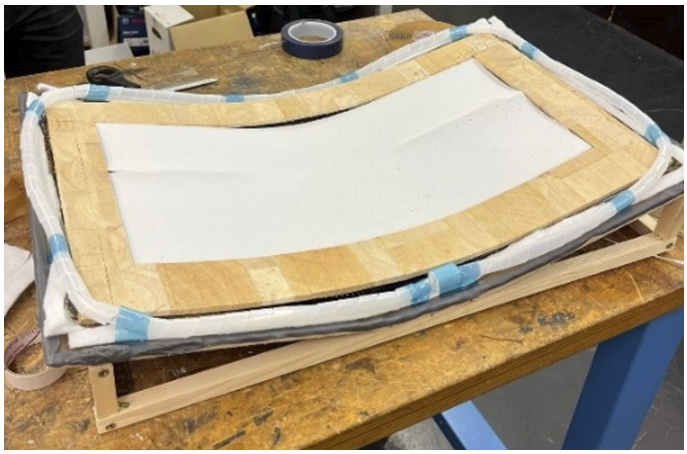

Figure 1.29: Construction of balsa wings at 1:4 scale

The wings weight for the same dimensions as the previous one is approximately the same. However, the stiffness seems this time more interesting, and the bending test was carried out in exactly the same way. We didn't manage at first to reach the breaking point because we were already at the bottom point, which led us to carry out several tests by adding more and more height. The test was therefore fairly conclusive and the part probably failed in fatigue rather than in pure bending. The values reached at the end of the first test were a displacement of 5cm for a force of 400N, i.e. 3 times more than the previous model.

#### 1.3.3.4 Final model

To determine the ideal model based on our previous simulations and experiments, we created a spreadsheet to calculate the weight of the infused terraces. Using this calculator, it was easy to change a parameter to deduce its influence. The final model was therefore defined by experiment, modifying one by one the thickness or surface of the different materials, while keeping an eye on the final weight, a criterion defined in the specifications as a maximum of 15kg.

The geometry was validated by testing, as it enabled us to save weight while retaining an interesting level of stiffness. We then incorporated a 5mm foam trampoline and 38mm balsa wingbars, the maximum thickness available on the market. The final model will also include 2 layers of basalt on each side (one at 0/90° and the inner layer at +/-45° for shear), as well as 3 plies of UD carbon (recovered from our school's waste) on each wingbar to increase stiffness. As the maximum stress is at the corner of the wingbar and not at its end, we have chosen to progressively reduce the size of the strips (1 , 2/3 and 1/3 of the width) to save weight, giving a predictive final weight of 14kg:

| échelle 1:1 Vfinal | basalte plain infusé | carbone UD infusé 1 | carbone UD infusé 2 | carbone UD infusé 3 | surface mousse infusée | wingbar balsa infusé | total |
|---|---|---|---|---|---|---|---|
| masse volumique (kg/m3) | 1836 | 2288,63 | 2288,63 | 2288,63 | 212,15 | 277,00 | |
| nombre de plis | 4 | 2 | 2 | 2 | 1 | 3 | |
| épaisseur (mm) | 0,668 | 0,4 | 0,4 | 0,4 | 5 | 38,1 | 39,97 |
| surface (m²) | 2,9 | 0,464 | 0,3312 | 0,2008 | 2,226 | 0,674 | |
| masse (kg) | 3,56 | 0,42 | 0,30 | 0,18 | 2,36 | 7,11 | 13,94 |

Figure 1.30: Wings weight calculations

### 1.3.4 Gantry

The creation of a fast female model based on our CAD model of the chassis presented above will enable us to validate our design under the effect of the various load cases established. To do this, we'll mesh our chassis into HEX3D elements, blocking the chassis attachment points according to the 6 DOFs and applying the loading described above to our model.

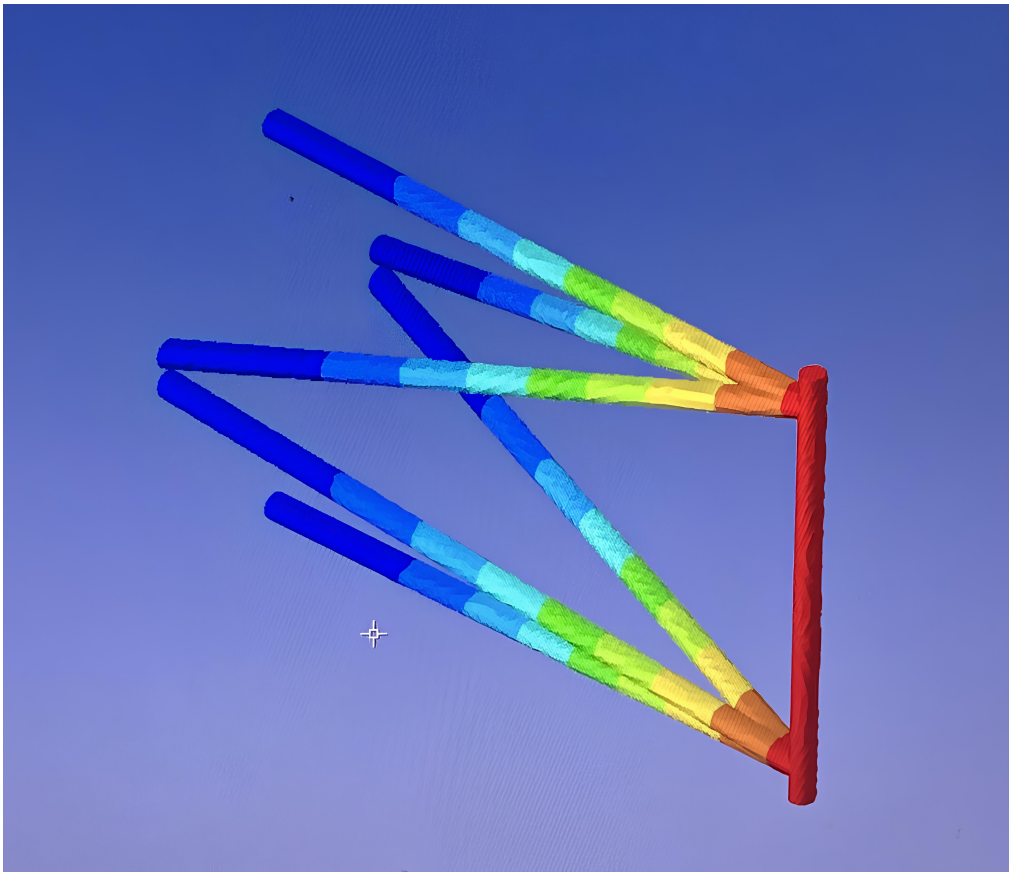

Figure 1.31: Chassis analysis

This analysis revealed perfectly admissible maximum displacements of the order of a few centimetres at most, and maximum stresses lower than the limit stresses in aluminum elasticity. The analysis also shows that the minimum safety coefficient of our model is of the order of 2.8. A perfectly acceptable margin according to our criteria, the model is therefore validated.

# Chapter 2

# Manufacturing and Cost analysis

## 2.1 Introduction

During the course of this project, we came to understand the importance of the manufacturing process and its direct impact on the design of the various elements. The most efficient design is rarely the simplest to implement, hence the importance of taking manufacturing into account right from the design phase. In this section, we will first look at the choices made to produce the wing and hull moulds. We will also detail the materials used and their SM$ equivalents.

## 2.2 Hull mould

After the CNC restoration we have made we decided to make the entire hull mould ourselves. This stage was a real challenge for a team that was still new to mould making. The machining capabilities of our machine were therefore a factor in our choice of manufacturing process. 3D machining and Z-axis travel were limiting factors. In addition, as explained in the hull design, the aim is to make a single mould using two axes of symmetry. The precision of the shape is therefore crucial to ensure the best possible assembly. That's why we decided to machine an MDF wood skeleton so that we could follow a precise shape during shaping and obtain a solid base while limiting ourselves to 2D machining. This structure is made up of several parts: 16 sections and a longitudinal part divided into 4. All these parts have notches so that they can be fitted together in position and then glued together.

We then filled each volume between the sections with 50kg/m3 PET foam, which we then

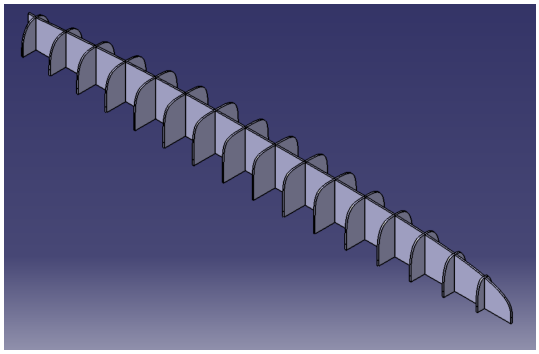

Figure 2.1: CAD of the skeleton mold (Catia V5)

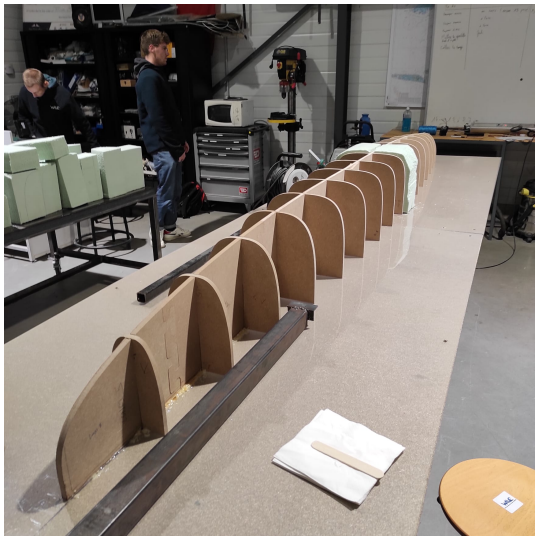

Figure 2.2: Assembled mould skeleton

shaped following the wooden skeleton. To further reduce our consumption of materials, we decided to use the positive mould directly for the infusion, so it had to be reinforced. To achieve this, 3 coats of 350g/m² basalt mat and a 115g/m² basalt plain to close the gaps were hand laid-up. To improve the surface finish we used resin filled with a mixture of hollow microspheres, which gave us a coating that was easy to sand.To ensure good demoulding we made sure to avoid 90° flat surfaces, so we added an angle of about 3° to the original design on these surfaces.

Figure 2.3: Reinforced mould with basalt laminates

## 2.3 Wings mould

Manufacturing wings is a complex and precise process requiring the use of well-designed molds. This part focuses on making a mold for wings using fir wood. Designing the angled wing mold is a critical step that requires careful planning. Sizing the mold is a key step in its manufacturing; it is necessary to have a precise mold, considering the necessary curves and angles to produce the cleanest part possible. It also seemed necessary to us to draw dimensioned plans from this modeling to be able to faithfully manufacture this mold. The entire design part of the mold was carried out on Catia.

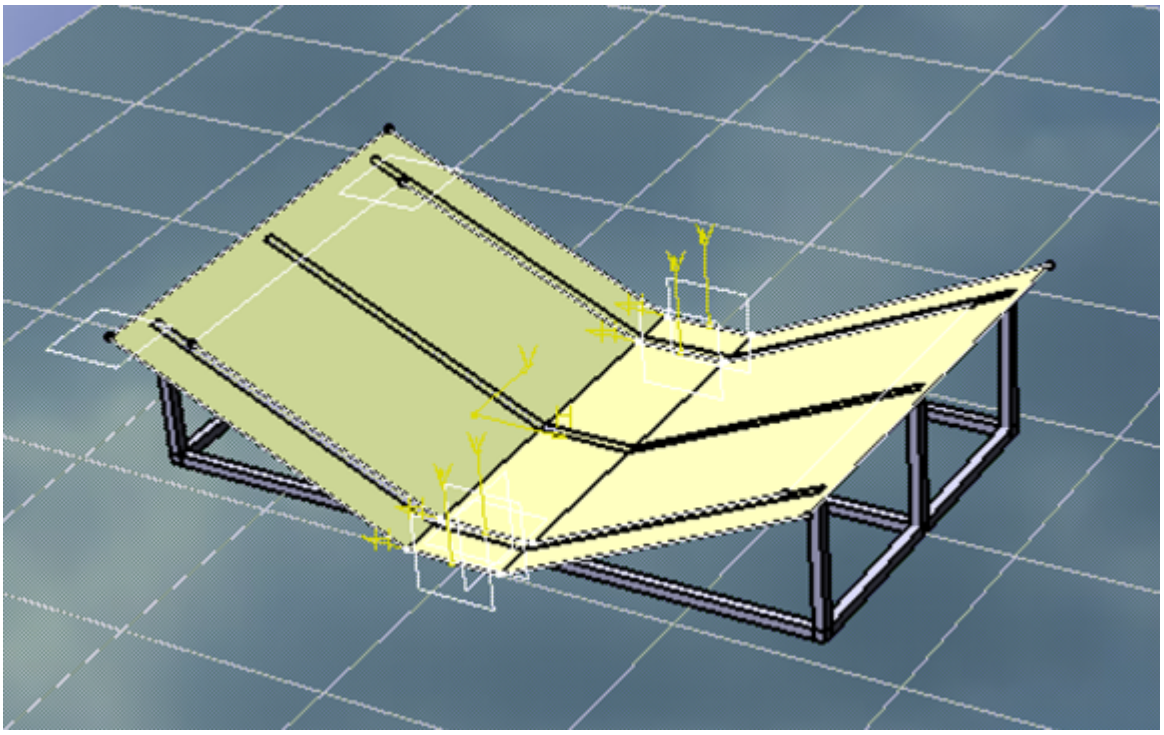

Figure 2.4: CAD of the wings mold (Catia)

It is essential that the mold is sufficiently robust to withstand the pressures exerted during the manufacturing process of the angled wings, while maintaining its shape and dimensions. In addition, given that the ecological and sustainable aspect are an integral part of the project, we decided to choose fir wood battens as well as plywood panels and not a simple folded metal sheet which would have been simpler to implement. The finishes were done using wood coating. We finally applied a Teflon film to the entire surface to be able to unmold the part as easily as possible.

Figure 2.5: Wings mold

## 2.4 Wings

In order to have the optimal resin/fibre ratio, we decided to use composite infusion process to manufacture the wings. Infusion of the part is the most crucial step in composite manufacturing. To avoid any problems during the manufacture, we carried out a study before the infusion. We first prepared the basalt fibres, the recycled PET foam as well as the basalt. During the first installation of the balsa pieces on the mold, we realized that the absence of a chamfer around this basalt would be problematic because it could generate preferential channels of resin at the intersection of the balsa and the foam underneath the fibres. These channels should absolutely be avoided because they cause local overflow of resin which results in an unnecessary increase in the weight of the part. We therefore decided to sand the balsa to get the cleanest infusion possible. Expanding foam was introduced then cut into the empty areas around the balsa. It is imperative to perfectly fill all the spaces otherwise the

resin could run into empty spaces which can generate an exothermic reaction and cause the infusion to fail and safety issues. Subsequently, we had to determine the resin injection paths. To infuse large pieces, as is the case with our terraces, it is necessary to define an optimized resin circulation path, allowing a homogeneous infusion of the materials. For this, we decided to place three resin injection pipes parallel to the front of the terrace, while drawing a vacuum around the periphery of the part. For practical reasons, we did not use fabrics woven at +/-45 degrees because it would have required three pieces to cover the terrace. Instead, we opted for 0/90 fabrics. Adding recovered carbon strips on the wingbars reinforced the structure against longitudinal forces, allowing us to use 0/90 fabrics in place of +/-45. To increase the stiffness of the side wingbar where the skipper will sit, we added a UD carbon strip during infusion. Additionally, we applied fillets around the balsa structures, which were not modeled in the FEM model. This not only ensured a cleaner infusion process but also contributed structurally by increasing the stiffness of the wingbars through added inertia.

## 2.5 Cost Analysis

| Wingbar mould | | | |
|---|---|---|---|
| Item | Quantity | Units | SuMoth dollars cost |
| Ply wood | 25.5 | kg | 0 |
| Wood beams | 20.3 | kg | 0 |
| Screws | 1.132 | kg | 11.32 |
| Total | | | 11.32 |

Figure 2.6: Wingbars mould cost analysis

| Wingbars | | | |
|---|---|---|---|
| Item | Quantity | Unites | SuMoth dollars cost |
| Basalt fiber | 2.85 | kg | 0 |
| Recycled PET Core | 1.5 | kg | 0 |
| CF UD strip (std modulus) | 0.35 | kg | 52.5 |
| Infusion greenepoxy | 9.8 | kg | 147 |
| Balsa | 3.7 | kg | 0 |
| Infusion mesh | 4.13 | square meters | 12.39 |
| Peel ply | 4.13 | square meters | 20.65 |
| Tacky tape | 1 | linear meters | 8 |
| Vacuum bagging | 6 | square meters | 12 |
| Spiral tubing | 6.1 | linear meters | 6.1 |
| PVC tubing | 18 | linear meters | 18 |
| Oven post cure | 24 | hours | 480 |
| Total | | | 756.64 |

Figure 2.7: Wingbars cost analysis

| Hull mould | | | |
|---|---|---|---|
| Item | Quantity | Units | SuMoth dollars cost |
| Basalt fiber | 4.5 | kg | 0 |
| PET Foam | 14.8 | kg | 0 |
| MDF wood | 50.6 | kg | 1012 |
| Laminating greenepoxy | 15 | kg | 225 |
| CNC | 1 | hours | 40 |
| Total | | | 1277 |

Figure 2.8: Hull mould cost analysis

| Rig | | | |
|---|---|---|---|
| Item | Quantity | Commercial cost | SuMoth dollars cost |
| Mast+Sail | 1 | 1500 | 0 |
| Total | | | 0 |

Figure 2.9: Rig cost analysis

| Total | |
|---|---|
| Item | SuMoth dollars cost |
| Wingbar mould | 11.32 |
| Wingbars | 756.64 |
| Hull mould | 1277 |
| Rig | 0 |
| Total | 2044.96 |

Figure 2.10: Total cost analysis

# Chapter 3

# Sustainability Assessment

In our journey towards participating in the Sumoth Challenge, we have placed a strong emphasis on sustainability assessment. Recognizing the critical need to minimize our environmental footprint, we have meticulously crafted our designs with this principle in mind.

One notable example is our approach to hull design, where we have implemented a symmetrical mold. This deliberate choice should not only enhances performance but also contributes to reducing environmental impact by optimizing material usage and minimizing waste.

While we acknowledge that there is always room for improvement, particularly in the efficiency of our manufacturing processes to decrease epoxy mastics consumption, we have taken proactive steps to address these challenges.

One such initiative involves the fabrication of essential tools using recycled materials. By crafting items like roller holders, a paint booth, and flexible sanding blocks in-house, we aim to mitigate resource consumption and promote reuse of materials readily available through recycling channels.

Through these conscientious efforts, we strive to embody sustainability principles at every stage of our project.

# Chapter 4

# Team

## 4.1 Team members

Here are the team members who contributed to the work done on the one and a half previous year. As many of them are going abroad or ending their master next year, a big turnover will occur and most of the roles will change.

**Team manager :** Guillaume DUMAS
**Captain :** Tanguy NOUEL
**Co-captain :** Brice BLOTTIERE
**Logistics officer :** Augustin LESTIENNE
**Communication officer :** Alexandre BERQUIN
**Sponsorship officer :** Mathéo GERARDIN

**Design:**

Amaury LECHAPELAIN

Théo ERKEL

Mathéo GERARDIN

Brice BLOTTIERE

**Control System:**

Guillaume DUMAS

Alexandre BERQUIN

Merlin CHARPY

Aubin BOCQUILLON

**Materials :**

Guillaume DUMAS

Tanguy NOUEL

Mathéo GERARDIN

Brice BLOTTIERE

**Life Cycle Analysis:**

Thomas LECHARTIER

Louis Weilbacher

Anthony Thibault

**Structure:**

Théo ERKEL

Brice BLOTTIERE

## 4.2 Sponsors


ESTACA
ECOLE D'INGENIEURS


RÉGION
PAYS
DE LA LOIRE


Lenovo


LANCELIN


IPC


ALTAIR


easycomposites


BASALTEX
The thread of stone

# Chapter 5

# Bibliography

[1] Rapport conception et construction durables, 11th Hour Racing Team, 2021.

[2] Cahier technique de l'innovation, Econav, 2010.

[3] Nautisme et composites biosourcés, Eurolarge Innovation, 2012.

[4] Sustainability, Bcomp, 2022.

[5] Architecture navale, Paulet, Presle, Neumann, 2020.